Proton Migration and Tautomerism in Protonated Triglycine

Christopher F. Rodriquez, Alwin Cunje, Tamer Shoeib, Ivan K. Chu, Alan C. Hopkinson, and K. W. Michael Siu*

Contribution from the Department of Chemistry and Centre for Research in Mass Spectrometry, York University, 4700 Keele Street, Toronto, Ontario, Canada M3J 1P3

Received May 9, 2000

Abstract: Proton migration in protonated glycylglycylglycine (GGG) has been investigated by using density functional theory at the B3LYP/6-31++G(d,p) level of theory. On the protonated GGG energy hypersurface 19 critical points have been characterized, 11 as minima and 8 as first-order saddle points. Transition state structures for interconversion between eight of these minima are reported, starting from a structure in which there is protonation at the amino nitrogen of the N-terminal glycyl residue following the migration of the proton until there is fragmentation into protonated 2-aminomethyl-5-oxazolone (the b_2 ion) and glycine. Individual free energy barriers are small, ranging from 4.3 to 18.1 kcal mol^{-1}. The most favorable site of protonation on GGG is the carbonyl oxygen of the N-terminal residue. This isomer is stabilized by a hydrogen bond of the type O−H···N with the N-terminal nitrogen atom, resulting in a compact five-membered ring. Another oxygen-protonated isomer with hydrogen bonding of the type O−H···O, resulting in a seven-membered ring, is only 0.1 kcal mol^{-1} higher in free energy. Protonation on the N-terminal nitrogen atom produces an isomer that is about 1 kcal mol^{-1} higher in free energy than isomers resulting from protonation on the carbonyl oxygen of the N-terminal residue. The calculated energy barrier to generate the b_2 ion from protonated GGG is 32.5 kcal mol^{-1} via **TS(6→7)**. The calculated basicity and proton affinity of GGG from our results are 216.3 and 223.8 kcal mol^{-1}, respectively. These values are 3−4 kcal mol^{-1} lower than those from previous calculations and are in excellent agreement with recently revised experimental values.

Introduction

Proton transfer between molecules has long been recognized as a fundamental process that plays an important role in many chemical reactions. In particular, proton migration across hydrogen bonds has been identified as the mechanism through which many biological functions are carried out.[1] Proton tunneling (hopping) has been postulated as the underlying mechanism for the activity of adenosine triphosphatase.[2] Proton transport in the gas phase has been examined largely as a means of assessing intrinsic proton migration chemistry in the absence of solvent effects.[3] The catalysis of intramolecular proton transfer between tautomers by a small neutral molecule has been the subject of several recent investigations.[4−7] For peptides, this type of catalysis could, in principle, be achieved by a neighboring basic functional group somewhere along the peptide backbone or in a side chain. The mechanism by which the proton migrates along a peptide backbone is not fully understood; the details of this mechanism are desirable to obtain fundamental insights into the chemistry of the peptide bond and also to probe the mechanism by which protonated peptides fragment in the gas phase.[8]

Fragmentation of protonated peptides is believed to be charge induced; the observation of a large number of product ions corresponding to fissure along a large number of the peptide bonds implies that there is a heterogeneous population of fragmenting peptide isomers and that interconversion between these isomers is likely to have low barriers and to be highly efficient.[8,9] On a peptide without basic side chains, the most favorable site of protonation in solution is the amino group of the N-terminus. A protonated peptide desorbed from the solution phase (having its proton at the N-terminus) would most likely isomerize to other structures in the gas phase. Indeed, a "mobile proton" model[9] has been postulated to account for the apparent mobility of the migrating proton in a peptide that results in a heterogeneous population of precursor ions differing primarily in the site of protonation. Furthermore, protonated peptide structures that fragment easily are those that are protonated on

* Address correspondence to this author. Phone: (416)650-8021. Fax: (416)736−5936. E-mail: kwmsiu@yorku.ca.

(1) Bountis, T., Ed. *Proton Transfer in Hydrogen-Bonded Systems*; NATO ASI Series B: Physics Vol. 291; Plenum Press: New York, 1992; pp 1−355.

(2) Senior, A. E. *Annu. Rev. Biophys. Biophys. Chem.* **1990**, *19*, 7−41.

(3) (a) Morton, T. H. *Tetrahedron* **1982**, *38*, 3195−3243. (b) McAdoo, D. J. *Mass Spectrom. Rev.* **1988**, *7*, 363−393. (c) Bowen, R. D. *Acc. Chem. Res.* **1991**, *24*, 364−371. (d) Longevialle, P. *Mass Spectrom. Rev.* **1992**, *11*, 157−192. (e) McAdoo, D. J.; Morton, T. H. *Acc. Chem. Res.* **1993**, *26*, 295−302. (f) Traeger, J. C.; Hudson, C. E.; McAdoo, D. J. *J. Mass Spectrom.* **1999**, *34*, 835−843.

(4) (a) Bohme, D. K. *Int. J. Mass Spectrom. Ion Processes* **1992**, *115*, 95−110. (b) Cunje, A.; Rodriquez, C. F.; Bohme, D. K.; Hopkinson, A. C. *J. Phys. Chem. A* **1998**, *102*, 478−483. (c) Cunje, A.; Rodriquez, C. F.; Bohme, D. K.; Hopkinson, A. C. *Can. J. Chem.* **1998**, *76*, 1138−1143. (d) Chalk, A. J.; Radom, L. *J. Am. Chem. Soc.* **1999**, *121*, 1574−1581.

(5) (a) Audier, H. E.; Leblanc, D.; Mourgues, P.; McMahon, T. B.; Hammerum, S. *J. Chem. Soc., Chem. Commun.* **1994**, 2329−2330. (b) Gauld, J. W.; Audier, H.; Fossey, J.; Radom, L. *J. Am. Chem. Soc.* **1996**, *118*, 6299−6300.

(6) (a) Gorb, L.; Leszczynski, J. *J. Am. Chem. Soc.* **1998**, *120*, 5024−5032. (b) Leszczynski, J. *J. Phys. Chem. A* **1998**, *102*, 2357−2362. (c) Gorb, L.; Leszczynski, J. *Int. J. Quantum Chem.* **1998**, *70*, 855−862. (d) Gu, J.; Leszczynski, J. *J. Phys. Chem. A* **1999**, *103*, 2744−2750.

(7) Rodriquez, C. F.; Cunje, A.; Shoeib, T.; Chu, I. K.; Hopkinson, A. C.; Siu, K. W. M. *J. Phys. Chem. A* **2000**, *104*, 5023−5028.

(8) Papayannopoulous, I. A. *Mass Spectrom. Rev.* **1995**, *14*, 49−73.

(9) (a) Jones, J. L.; Dongre, A. R.; Somogyi, A.; Wysocki, V. H. *J. Am. Chem. Soc.* **1994**, *116*, 8368−8369. (b) Dongre, A. R.; Jones, J. L.; Somogyi, A.; Wysocki, V. H. *J. Am. Chem. Soc.* **1996**, *118*, 8365−8374. (c) Dongre, A. R.; Somogyi, A.; Wysocki, V. H. *J. Mass Spectrom.* **1996**, *31*, 339−350.

10.1021/ja0015904 CCC: $20.00
Published on Web 03/07/2001

the amide nitrogen atoms, as this weakens the amide bond and makes fragmentation energetically favorable. The experimental evidence in support of this model is compelling.[10] Despite the model's apparent popularity, the isomerization mechanism upon which it is based and proton migration in peptides have never been rigorously examined, even for a simple protonated tripeptide. Here we report the first detailed theoretical investigation of this proton migration and tautomerism using density functional theory calculations.

The tripeptide glycylglycylglycine, GGG, is the simplest model peptide that reproduces many of the structural features of larger peptides and proteins. Accurate ab initio molecular orbital calculations on protonated triglycine are computationally expensive, and they cannot be performed easily on workstations at the present time. The first six critical points, all minima, on the potential energy hypersurface of protonated GGG have been reported by Zhang et al.[11] by using ab initio methods (HF/6-31G(d)//HF/6-31G(d)). Their calculated proton affinity (PA) of 227.9 kcal mol^{-1} and gas-phase basicity (GB) of 219.6 kcal mol^{-1} can be compared with recently revised experimental results[12] of 224.7 ± 0.5 and 216.6 ± 0.5 kcal mol^{-1}, respectively. In a more recent study by Strittmatter and Williams[12] at the B3LYP/6-31G(d)//SVWN/6-31G(d) level of theory, a comparable result for the proton affinity of GGG (227.8 kcal mol^{-1}) was reported. Two additional structures were characterized to be at minima: one is at the lowest energy minimum for neutral GGG and the other is at the lowest energy minimum for protonated GGG.

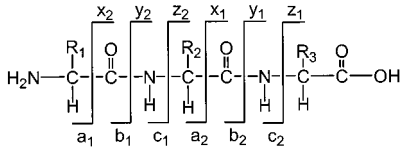

The primary structure or sequence of amino acid residues in peptides can be probed by studying the CID (collision induced dissociation) reactions of the protonated peptides. As discussed earlier, it is believed that fragmentation of protonated peptides in the gas phase occurs at the peptide bond proximal to the proton. If charge retention is on the N-terminal fragment then a b_n ion is produced. Alternatively, if charge retention is on the C-terminal fragment then the y_n ion is generated. Other peptide fragments include a_n ions, immonium ions, and ions corresponding to the loss of small neutrals, such as $[M + H - H_2O]^+$, $[M + H - CO]^+$, and $[M + H - NH_3]^+$. Under low-energy CID conditions, there have been several studies[13] on the major fragment ions of protonated glycine oligomers from protonated diglycine (G_2H^+) to protonated pentaglycine (G_5H^+). In G_2H^+ the major fragment ion is the y_1 while for G_3H^+ it is the b_2.[13g] In the case of the G_4H^+ and G_5H^+ fragmentation spectra, the emergence of the $[M + H - H_2O]^+$ ion can be clearly seen and is of comparable intensity to the b- and y-type ions.

There is a consensus among experimentalists that the b-type ions have a protonated 2-substituted-5-oxazolone structure.[13e,f,14] An immonium ion isomer has been proposed as a possible alternative structure for the b_2 ion;[15] this structure, however, was found to be unnecessary in a recent mechanistic study.[14a] Theoretically, an abbreviated form of a protonated dipeptide without side chains, $HC(O)NHCH_2C(O)NH_3^+$, was investigated to determine the reaction mechanism for b_2 ion generation and to investigate proton mobility.[16] In the first step the amide bond, $HC(O)NHCH_2C(O)\cdots NH_3^+$, breaks and ring closure takes place simultaneously to form an ion−neutral complex consisting of a protonated oxazolone and ammonia.[16a] The barrier to this reaction, starting from the high-energy N-protonated tautomer, is only 9.5, 10.5, and 10.1 kcal mol^{-1} at the G2MP2, MP2/6-31G(d,p), and B3LYP/6-31G(d,p) levels of theory, respectively. The ion−neutral complex then decomposes to the b_2 ion and ammonia, a process that requires about 15 kcal mol^{-1}. However, this abbreviated dipeptide model cannot replicate the kinetic properties of larger peptides. In the mobile proton model, the proton is shuttled along the amide linkages to arrive at the site of fragmentation. Therefore, this dipeptide that contains two atypical amide linkages is not a very satisfactory model in which to investigate the reaction mechanisms of b_n ions in larger peptides. The smallest tripeptide, GGG, can be used in this regard and with the advent of more robust scalable computers, the profile of the protonated GGG potential energy hypersurface is now accessible at a reliable level of theory.

Recently, we have investigated the structures of neutral and protonated 2-aminomethyl-5-oxazolone, 2-aminomethyl-4-methyl-5-oxazolone, 2-phenyl-5-oxazolone, and 2-phenyl-4-methyl-5-oxazolone, at B3LYP/6-31++G(d,p).[17] Standard enthalpies of formation were calculated at both MP4SDTQ/6-311++G-(2df,p)//B3LYP/6-31++G(d,p), using the atomization method, and B3LYP/6-31++G(d,p), using isodesmic equations, for neutral and N-protonated 2-aminomethyl-5-oxazolone. In another study, we calculated the free energy barrier to the 1,3-proton shift, moving the migrating proton from the carbonyl oxygen to the nitrogen atom of the C-terminal amide bond in triglycine, at B3LYP/6-31++G(d,p).[7] This barrier, at 39.6 kcal mol^{-1}, is significant and probably not a likely route in forming the b_2 ion. However, in the presence of water, the free energy barrier is reduced to 26.7 kcal mol^{-1} and is further reduced in methanol to 22.0 kcal mol^{-1}. In this current investigation, using B3LYP/6-31++G(d,p) calculations for protonated triglycine, we investigate proton transport and tautomerism in protonated peptides by presenting a reaction mechanism involving the transfer of a proton from the terminal $-NH_3^+$ group to the

(10) (a) Tsapralis, G.; Nair, H.; Somogyi, A.; Wysocki, V. H.; Zhong, W.; Futrell, J. H.; Summerfield, S. G.; Gaskell, S. J. *J. Am. Chem. Soc.* **1999**, *121*, 5142−5154. (b) Gu, C.; Somogyi, A.; Wysocki, V. H.; Medzihradsky, K. F. *Anal. Chim. Acta* **1999**, *397*, 247−256. (c) Harrison, A. G.; Yalcin, T. *Int. J. Mass Spectrom. Ion Processes* **1997**, *165−167*, 339−347. (d) Mueller, D. R.; Eckersley, M.; Richter, W. *Org. Mass Spectrom.* **1988**, *23*, 217−222. (e) Johnson, R. S.; Krylov, D.; Walsh, K. A. *J. Mass Spectrom.* **1995**, *30*, 368−387. (f) Vaisar, T.; Urban J. *J. Mass Spectrom.* **1998**, *33*, 505−524.

(11) Zhang, K.; Cassady, C. J.; Chung-Phillips, A. *J. Am. Chem. Soc.* **1994**, *116*, 11512−11521.

(12) Strittmatter, E. F.; Williams, E. R. *Int. J. Mass Spectrom.* **1999**, *185/186/187*, 935−948.

(13) (a) Yeh, R. W.; Grimley, J. M.; Bursey, M. M. *Biol. Mass Spectrom.* **1991**, *20*, 443−450. (b) Morgan, D. G.; Bursey, M. M. *Biol. Mass Spectrom.* **1993**, *22*, 502−510. (c) Morgan, D. G.; Bursey, M. M. *Org. Mass Spectrom.* **1994**, *29*, 354. (d) Morgan, D. G.; Bursey, M. M. *J. Mass Spectrom.* **1995**, *30*, 290. (e) Yalcin, T.; Khouw, C.; Csizmadia, I. G.; Peterson, M. B.; Harrison, A. G. *J. Am. Soc. Mass Spectrom.* **1995**, *6*, 1164−1174. (f) Yalcin, T.; Csizmadia, I. G.; Peterson, M. B.; Harrison, A. G. *J. Am. Soc. Mass Spectrom.* **1996**, *7*, 233−242. (g) Reid, G. E.; Simpson, R. J.; O'Hair, R. A. J. *Int. J. Mass Spectrom.* **1999**, *190/191*, 209−230. (h) Reid, G. E.; Simpson, R. J.; O'Hair, R. A. J. *J. Am. Soc. Mass Spectrom.* **1998**, *9*, 945−956. (i) Klassen, J. S.; Kebarle, P. *J. Am. Chem. Soc.* **1997**, *119*, 6552−6563.

(14) (a) Harrison, A. G.; Csizmadia, I. G.; Tang, T.-H *J. Am. Soc. Mass Spectrom.* **2000**, *11*, 427−436. (b) Cordero, M. M.; Houser, J. J.; Wesdemiotis, C. *Anal. Chem.* **1993**, *65*, 1594−1601. (c) Nold. M. J.; Wesdemiotis, C.; Yalcin, T.; Harrison, A. G. *Int. J. Mass Spectrom. Ion Processes* **1997**, *164*, 137−153. (d) Cordero, M. M.; Wesdemiotis, C. *Org. Mass Spectrom.* **1994**, *29*, 382−386.

(15) Eckart, K.; Holthausen, M. C.; Koch, W.; Spiess, J. *J. Am. Soc. Mass Spectrom.* **1998**, *9*, 1002−1011.

(16) (a) Paizs, B.; Lendavy, G.; Vekey, K.; Suhai, S. *Rapid Commun. Mass Spectrom.* **1999**, *13*, 525−533. (b) Csonka, I. P.; Paizs, B.; Lendvay, Suhai, S. *Rapid Commun. Mass Spectrom.* **2000**, *14*, 417−431.

(17) Rodriquez, C. F.; Shoeib, T.; Chu, I. K.; Siu, K. W. M.; Hopkinson, A. C. *J. Phys. Chem. A* **2000**, *104*, 5335−5342.

nitrogen atom of the C-terminal amide bond, followed by formation of the protonated 2-aminomethyl-5-oxazolone and glycine. We also show that, when free energies are used rather than enthalpies, the *most favorable site of protonation is not the N-terminal nitrogen atom but the carbonyl oxygen atom of the first residue*.

Methods

All calculations were performed with Gaussian 98[18] on a Silicon Graphics Origin 2000 with 16 processors and 8 GB of memory. Density functional theory at the B3LYP level, in conjunction with the 6-31++G(d,p) basis set, was employed for structure optimizations and for the characterization of critical points by using harmonic vibrational frequencies.[19] Estimated structures for the transition states were determined by using the QST2 method.[18] First-order saddle points were then found by using the Berny transition state algorithm and the CalcAll method.[18]

Long weak bonds are particularly difficult to describe by molecular orbital theory. Nevertheless, density functional theory calculations employing hybrid functionals such as B3LYP appear to describe hydrogen bonding accurately in smaller systems such as water dimers and complexes,[20] hydrogen fluoride dimers,[21] and clusters of hydrogen cyanide and cyanoacetylene.[22] Our work here provides the first calculations, employing the hybrid functional B3LYP in conjunction with the 6-31++G(d,p) basis set, on computationally large peptides where hydrogen bonding is an intrinsic structural property. Descriptions of transition state structures also contain long bonds and potentially suffer from similar difficulties. However, by using a hybrid DFT functional such as B3LYP, the enthalpies of activation for proton transfer are comparable to those at MP2.[16b,20b] Within our group, there are several examples[4b,c,7] showing that calculations at B3LYP/6-31++G(d,p) and B3LYP/6-311++G(d,p)give comparable enthalpies of activation to those from QCISD(T)/6-311++G(2df,p) and CCSD-(T)/6-311++G(2df,p) calculations.

Results and Discussion

The Neutral Structures. Structures **N1**−**N3**, **P1**, **1**−**10**, and all transition structures are shown in Figure 1 and their total energies, zero-point vibrational terms, and entropies are given in Table 1s in the Supporting Information. The relative electronic energies, enthalpies, and free energies at 298 K are displayed in Table 1.

Table 1. Relative Electronic Energies, Enthalpies, and Free Energies of Structures (all in kcal mol^{-1})

structure	rel energies	rel enthalpies	rel free energies
N1	231.9	224.2	215.0
N2	231.9	224.2	215.0
N3	234.8	226.6	215.2
P1	−0.1	−0.1	0.4
1	0.0	0.0	0.0
2	1.8	0.4	−1.3
3	8.2	6.7	4.3
4	2.0	−0.2	−1.2
5	16.8	15.4	14.0
6	21.4	19.1	17.5
7	31.3	29.3	25.3
7′	17.6	14.9	12.3
8	39.4	35.2	23.2
9	15.9	14.4	13.3
10	16.6	16.0	15.5
TS(1→2)	7.5	4.3	4.3
TS(2→3)	14.6	12.6	11.1
TS(3→4)	14.3	11.9	11.0
TS(4→5)	18.7	16.9	16.9
TS(5→6)	21.6	17.4	16.9
TS(6→7)	34.6	32.1	31.3
TS(9→6)	58.2	53.6	53.0
TS(10→2)	45.5	41.6	41.9

The HF/6-31G(d) results of Zhang et al.[11] were used to provide initial structures for our geometric optimizations of neutral and protonated GGG calculated at B3LYP/6-31++G-(d,p). The resulting structures were then modified to produce various isomers of protonated GGG that could be found on the energy hypersurface, thereby providing the pathway for a mechanism to generate the b_2 ion. In our endeavor to locate the lowest energy structures of both neutral and protonated GGG, many isomers were optimized. Only the lowest energy structures are shown here. We were able to optimize and characterize three isomers of neutral GGG; two, **N1** and **N2**, are folded structures, whereas the third, **N3**, is a linear system. The neutral **N2** is our optimized structure employing the lowest energy HF/6-31G(d) minimum of Zhang et al.[11] as the initial structure. The only significant difference between the two structures is the distance between the N-terminal amino hydrogen and the C-terminal carbonyl oxygen atoms. In the lowest energy structure of Zhang et al. that distance is 2.654 Å, whereas in our **N2** it is 3.683 Å. This difference is probably due to the more accurate description of long-range interactions in our higher level of theory, B3LYP/6-31++G(d,p), in which electron correlation and diffuse functions are incorporated. Of our three structures, **N2** is also the one closest to the optimized structure for neutral GGG (via molecular mechanics) of Strittmatter and Williams;[12] the major difference is the orientation of the COOH group. Our lowest energy neutral structures, **N1** and **N2,** are 2.9 kcal mol^{-1} (Table 1) below **N3**. When enthalpy differences at 298 K are considered, the results remain essentially unchanged. However, when the entropy terms are introduced, there is only a *0.2 kcal mol^{-1} difference* in free energies among the three isomers. That is to say the differences in free energies are negligible.

Energy Hypersurface Adjusted by the Addition of Entropy To Provide Relative Free Energies. The mechanistic pathway for transfer of a proton from the N-terminal nitrogen

(18) (a) *Gaussian 98*, revision A.6; Frisch, M. J.; Trucks, G. W.; Schlegel, H. B.; Scuseria, G. E.; Robb, M. A.; Cheeseman, J. R.; Zakrzewski, V. G.; Montgomery, J. A., Jr.; Stratmann, R. E.; Burant, J. C.; Dapprich, S.; Millam, J. M.; Daniels, A. D.; Kudin, K. N.; Strain, M. C.; Farkas, O.; Tomasi, J.; Barone, V.; Cossi, M.; Cammi, R.; Mennucci, B.; Pomelli, C.; Adamo, C.; Clifford, S.; Ochterski, J.; Petersson, G. A.; Ayala, P. Y.; Cui, Q.; Morokuma, K.; Malick, D. K.; Rabuck, A. D.; Raghavachari, K.; Foresman, J. B.; Cioslowski, J.; Ortiz, J. V.; Stefanov, B. B.; Liu, G.; Liashenko, A.; Piskorz, P.; Komaromi, I.; Gomperts, R.; Martin, R. L.; Fox, D. J.; Keith, T.; Al-Laham, M. A.; Peng, C. Y.; Nanayakkara, A.; Gonzalez, C.; Challacombe, M.; Gill, P. M. W.; Johnson, B. G.; Chen, W.; Wong, M. W.; Andres, J. L.; Head-Gordon, M.; Replogle, E. S.; Pople, J. A.; Gaussian, Inc.: Pittsburgh, PA, 1998. (b) *Gaussian 98*, revision A.5; Frisch, M. J.; Trucks, G. W.; Schlegel, H. B.; Scuseria, G. E.; Robb, M. A.; Cheeseman, J. R.; Zakrzewski, V. G.; Montgomery, J. A., Jr.; Stratmann, R. E.; Burant, J. C.; Dapprich, S.; Millam, J. M.; Daniels, A. D.; Kudin, K. N.; Strain, M. C.; Farkas, O.; Tomasi, J.; Barone, V.; Cossi, M.; Cammi, R.; Mennucci, B.; Pomelli, C.; Adamo, C.; Clifford, S.; Ochterski, J.; Petersson, G. A.; Ayala, P. Y.; Cui, Q.; Morokuma, K.; Malick, D. K.; Rabuck, A. D.; Raghavachari, K.; Foresman, J. B.; Cioslowski, J.; Ortiz, J. V.; Stefanov, B. B.; Liu, G.; Liashenko, A.; Piskorz, P.; Komaromi, I.; Gomperts, R.; Martin, R. L.; Fox, D. J.; Keith, T.; Al-Laham, M. A.; Peng, C. Y.; Nanayakkara, A.; Gonzalez, C.; Challacombe, M.; Gill, P. M. W.; Johnson, B. G.; Chen, W.; Wong, M. W.; Andres, J. L.; Head-Gordon, M.; Replogle, E. S.; Pople, J. A.; Gaussian, Inc.: Pittsburgh, PA, 1998.

(19) (a) Becke, A. D. *Phys. Rev. A* **1988**, *38*, 3098−3100. (b) Becke, A. D. *J. Chem. Phys.* **1993**, *98*, 5648−5652. (c) Lee, C.; Yang, W.; Parr, R. G. *Phys. Rev. B* **1988**, *37*, 785−789. (d) Ditchfield, R.; Hehre, W. J.; Pople, J. A. *J. Chem. Phys.* **1971**, *54*, 724−728. (e) Hehre, W. J.; Ditchfield, R.; Pople, J. A. *J. Chem. Phys.* **1972**, *56*, 2257−2261. (f) Hariharan, P. C.; Pople, J. A. *Mol. Phys.* **1974**, *27*, 209−214. (g) Gordon, M. S. *Chem. Phys. Lett.* **1980**, *76*, 163−168. (h) Hariharan, P. C.; Pople, J. A. *Theor. Chim. Acta* **1973**, *28*, 213−222. (i) Clark, T.; Chandrasekhar, J.; Spitznagel, G. W.; Schleyer, P. v. R. *J. Comput. Chem.* **1983**, *4*, 294−301.

(20) (a) Topol, I. A.; Burt, S. K.; Rashin, A. A. *Chem. Phys. Lett.* **1995**, *247*, 112−119. (b) Barone, V.; Orlandini, L.; Adamo, C. *Chem. Phys. Lett.* **1994**, *231*, 295−300.

(21) Latajka, Z.; Bouteiller, Y. *J. Chem. Phys.* **1994**, *101*, 9793−9799.

(22) Karpfen, A. *J. Phys. Chem.* **1996**, *100*, 13474−13486.

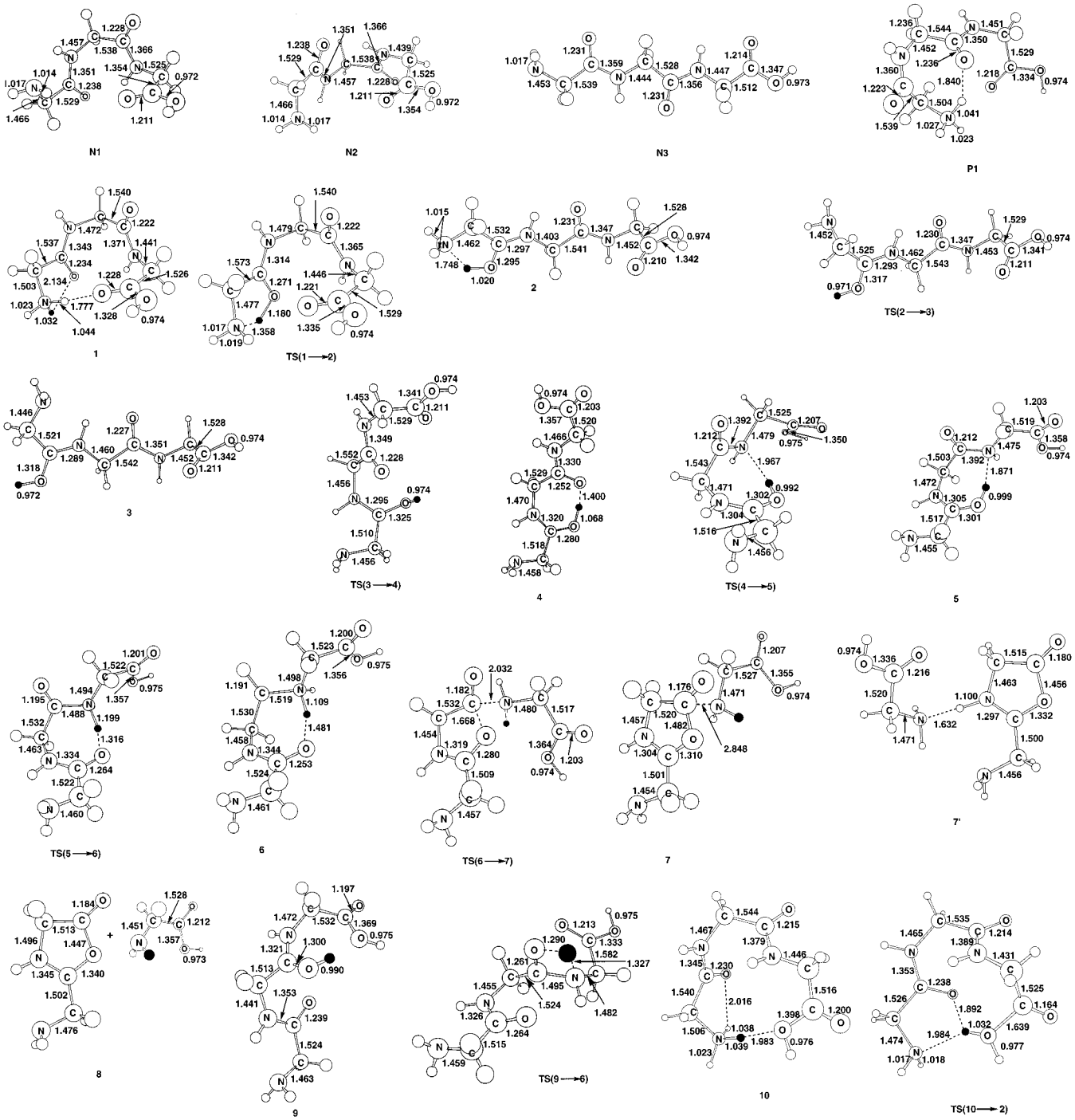

Figure 1. Optimized structures at B3LYP/6-31++G(d,p) with bond lengths in angstroms and bond angles in degrees. The migrating proton is the filled black circle in the diagrams.

to the amide nitrogen of the C-terminal peptide bond and subsequent cleavage to form the b_2 ion is provided in Scheme 1. The relative free energies of structures involved in this mechanism are shown in Figure 2. In protonated triglycine, there is sufficient structural flexibility to form long-range hydrogen bonds. There are four basic types of hydrogen bonding interactions in peptides, all involving combinations of N and O atoms: N−H···N, O−H···N, N−H···O, and O−H···O. In the structures, we have arbitrarily drawn dotted lines and reported distances only when X···H is less than 2.0 Å.

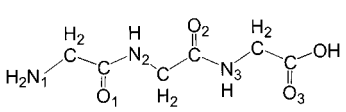

For protonated triglycine, two low-energy N-terminal nitrogen-protonated structures, **P1** and **1**, have been found. Structure **1** is lower in energy than **P1** by only 0.4 kcal mol^{-1}. Structure **1** is similar to the lowest energy structure found by Zhang et al.,[11] whereas **P1** is closer to the optimized structure of Strittmatter and Williams.[12] In **P1**, a hydrogen bond, 1.840 Å in length, of the type $N_1-H\cdots O_2$ (the subscripts refer to the residue number) provides stability, while in **1** calculations indicate a shorter hydrogen bond, 1.777 Å, of the type $N_1-H\cdots O_3$. Using this hydrogen bond in **P1**, the proton on the amino nitrogen can be transferred to the carbonyl oxygen (O_2) of the second peptide bond. This has a major disadvantage as regards to the formation of the b_2 ion, as the barrier to a subsequent 1,3-proton-transfer

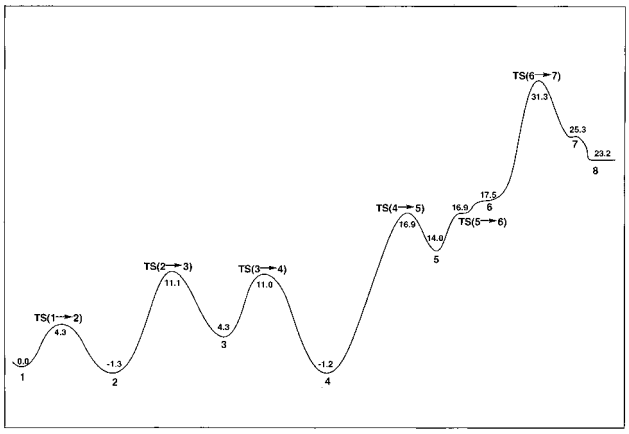

Figure 2. Energy profile corrected to bear free energy values at B3LYP/6-31++G(d,p) in kcal mol^{-1} for the protonation of GGG and the subsequent fragmentation to yield protonated 2-aminomethyl-5-oxazolone and glycine.

Scheme 1

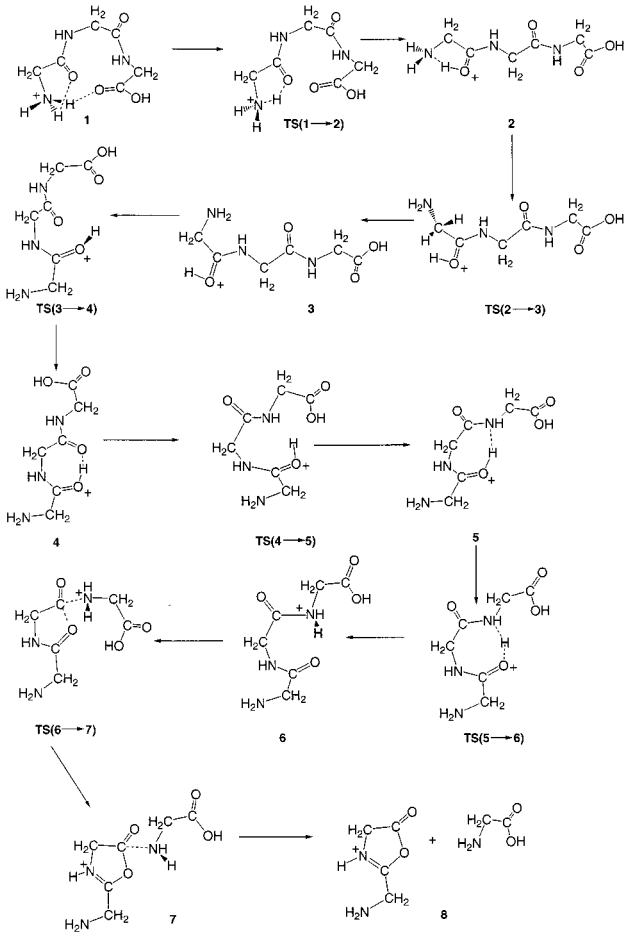

shift to place the proton on the amide nitrogen (N_3), required for fragmentation to occur, is approximately 40 kcal mol^{-1}.[7]

In **1**, the migrating proton on the amino nitrogen can easily be transferred by taking advantage of a $N_1-H\cdots O_1$ long-range hydrogen bond of 2.134 Å to produce structure **2**. The energy barrier to this 1,4-proton transfer via **TS(1→2)** is only 4.3 kcal mol^{-1}. *Structure* **2** *is actually at the global minimum* on our calculated energy surface, and is lower in free energy than **1** by 1.3 kcal mol^{-1}. To our knowledge, there have been no previous calculations on this structure. It is an unexpectedly stable structure as it has unfolded from **1** to produce an almost linear ion. The entropy contribution for a linear system such as **2** is larger than that from a folded structure. One of the major structural contributions to the stability of **2** is the short hydrogen bond ($O_1-H\cdots N_1$) of 1.748 Å. The resulting five-membered ring in **2** is more compact (shorter bond lengths) than the analogous ring in **1**. Furthermore, protonation on the carbonyl oxygen in **2** allows the charge to be dispersed to the amide nitrogen.[7]

To produce a structure in the form of the protonated 2-aminomethyl-5-oxazolone, **8**, it is then necessary to rotate the N-terminal amino group to be trans to the carbonyl oxygen group ($\angle N_1CCO_1 \approx 180°$). Structure **3** produced from this rotation is 4.3 kcal mol^{-1} higher in energy than **1**. The transition structure, **TS(2→3)**, for the rotation is 12.4 kcal mol^{-1} above **2**. The migrating proton now located on O_1 can also interact with the oxygen atom (O_2) of the other amide bond; to achieve this the CO_1H^+ group as well as some of the bonds on the peptide backbone must rotate, via **TS(3→4),** to produce **4**. The barrier to these simultaneous rotations, 6.7 kcal mol^{-1}, is small and structure **4** *is only 0.1 kcal mol^{-1} higher in free energy than the structure at the global minimum,* **2**. Structure **4** contains a seven-membered ring with a $CO_1-H\cdots O_2C$ hydrogen bond of 1.400 Å, the shortest one found on this hypersurface. In **4**, some of the positive charge is delocalized onto the adjacent amide bond as shown by the length of the C_2-N_3 bond that has decreased from 1.351 to 1.330 Å. This protonated triglycine structure has never been reported in the literature. However, interactions of the O−H···O type on glycylglycine have been found with use of AM1.[23] Subsequent HF/STO-3G calculations, however, revealed that in a dipeptide this type of structure is a transition state and not at a minimum.[24]

The next step requires a major conformational rearrangement and the isomerization barrier from **4** to **5**, via **TS(4→5)**, is relatively high at 18.1 kcal mol^{-1}. Structure **5** lies 14.0 kcal mol^{-1} above **1**. The migrating proton in **5** is now involved in a hydrogen-bonded interaction of the type $O_1-H\cdots N_3$ (at a length of 1.871 Å) and is in an ideal position to be transferred onto the amide nitrogen atom of the second peptide linkage. The transition state for this process is **TS(5→6)**; the associated product minimum is structure **6**, which is 17.5 kcal mol^{-1} higher in free energy than **1** (Table 1). **TS(5→6)** is only 0.2 kcal mol^{-1} higher in electronic energy than structure **6**. This is a very small difference and is a reflection of the similarities in their structures. When zero-point vibrational energies, thermal corrections, and entropies are included, **TS(5→6)** is actually lower in (free) energy than structure **6**. Cases such as this are not unusual,[25] and it explains the section of the energy profile between **5**, **TS(5→6)**, and **6**. Clearly then, the barrier for converting structure **5** to **6** is simply the endoergicity of the reaction.

Structure **6** now has the proton on the nitrogen atom of the amide linkage where fragmentation occurs. This amide bond has lengthened from 1.392 Å in **5** to 1.519 Å in **6**, indicating a weakening of the bond. Conversion of **6** into **7** via **TS(6→7)** requires 13.8 kcal mol^{-1}. In this transition structure, the motions associated with the single imaginary vibrational frequency are for concerted formation of the oxazolone ring and dissociation of the amide bond. The associated minimum, **7**, is an ion−neutral complex with a long ion−neutral bond of 2.848 Å. This

(23) (a) Wu, J.; Lebrilla, C. B. *J. Am. Chem. Soc.* **1993**, *115*, 3270−3275. (b) Wu, J.; Gard, E.; Bregar, J.; Green, M. K.; Lebrilla, C. B. *J. Am. Chem. Soc.* **1995**, *117*, 9900−9905.

(24) Zhang, K.; Zimmerman, D. M.; Chung-Phillips, A.; Cassady, C. J. *J. Am. Chem. Soc.* **1993**, *115*, 10812−10822.

(25) (a) Rodriquez, C. F.; Bohme, D. K.; Hopkinson, A. C. *J. Am. Chem. Soc.* **1993**, *115*, 3263−3269. (b) Rodriquez, C. F.; Bohme, D. K.; Hopkinson, A. C. *J. Org. Chem.* **1993**, *58*, 3344−3349.

Scheme 2

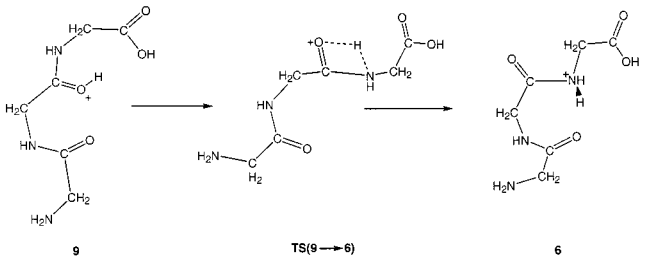

Scheme 3

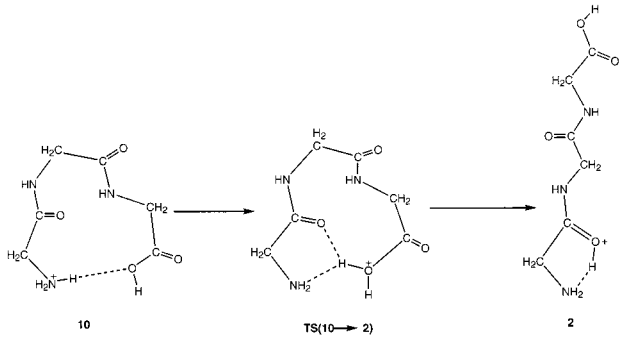

structure is 25.3 kcal mol^{-1} above **1**. There is no barrier to dissociation from structure **7** to **8**, the final product which lies 23.2 kcal mol^{-1} above **1**. It is also noteworthy that there is another ion−neutral complex, **7′**, that is 13.0 kcal mol^{-1} lower in energy than **7**. In structure **7′** the amino nitrogen of glycine is now hydrogen bonded to the most acidic hydrogen (the one on the ring nitrogen) of protonated oxazolone.

An alternative mechanistic route would involve transferring the migrating proton in structure **4** from the carbonyl oxygen of the first residue to that of the second residue to yield structure **9**, which is 13.3 kcal mol^{-1} higher in free energy than **1**. This would be followed by transfer of the proton to the amide nitrogen, a 1,3-proton shift via **TS(9→6)**, but the barrier to such a shift, 39.6 kcal mol^{-1}, is considerable (Scheme 2).[7] **TS(9→6)** is 53.0 kcal mol^{-1} higher in free energy than **1**; this high overall barrier renders this alternative process noncompetitive versus the lower energy route that proceeds through **TS(6→7)**, and has an energy barrier of only 31.3 kcal mol^{-1} above **1**.

Under collisionally activated decomposition conditions there is sufficient energy (typically 2−3 eV) to overcome the small barriers between **1** and **4**. When the site of protonation is the carbonyl oxygen as in **4**, there is *an energy barrier of only 32.5 kcal mol^{-1}*, via **TS(6→7)**, to the final products, the b_2 ion and glycine. The magnitude of this barrier is consistent with the experimental results of Klassen and Kebarle,[13i] who employed threshold-energy measurements to yield an estimate of the activation energy at 54.5 kcal mol^{-1}. This value, however, is only an upper limit of the activation energy as the kinetic shift, which is large for an ion with as many bonds as protonated triglycine, was ignored. Incorporation of the kinetic shift will reduce this estimate drastically.[13i]

Although the generation of the $[M + H - H_2O]^+$ ion is negligible in the fragmentation of protonated triglycine, we tried to calculate the transition structure that is involved in the direct transfer of the proton from structure **10**, 15.5 kcal mol^{-1} above structure **1,** to the hydroxyl group at the C-terminus (Scheme 3). The transition structure **TS(10→2)**, 41.9 kcal mol^{-1} above structure **1**, bears a resemblance to this process; the proton is located on the oxygen atom of the hydroxy group with an OH bond length of 1.032 Å and the C···H_2O bond length is strikingly long, 1.639 Å. An Intrinsic Reaction Coordinate (IRC) calculation on this transition structure established that the product derived from this transition state is not that resulting from the loss of H_2O, but rather structure **2**, i.e., the OH group functions as a catalyst for an internal proton transfer from structure **10** to **2**.

Calculated Proton Affinities and Gas-Phase Basicities. A large number of studies have been devoted to investigating the most probable protonation site on a peptide.[11,12,13a,b,23,24,26] We have shown in the previous section that structure **1** (GGG protonated on the amino nitrogen) is about 1 kcal mol^{-1} higher in free energy than structure **2** (GGG protonated on the carbonyl oxygen of the first residue plus intramolecular solvation by the amino nitrogen) and structure **4** (GGG protonated on the carbonyl oxygen of the N-terminal amide group stabilized by intramolecular hydrogen bonding to the carbonyl oxygen of the second residue). It should be noted that the relative stability of **2** is a consequence of its larger entropy; on the potential energy hypersurface **1** is *lower* in energy than **2** by 0.4 kcal/mol.

The gas-phase basicity of a base B is the free-energy change, $\Delta G°_{r,298}$, whereas the proton affinity is the enthalpy change, $\Delta H°_{r,298}$, of reaction 1.

$$BH^+ \rightarrow B + H^+ \quad (1)$$

The gas-phase basicity and the proton affinity of B are linked by

$$\Delta G°_{r,298} = \Delta H°_{r,298} - T\Delta S_{r,298} \quad (2)$$

$\Delta H°_{r,298}$ may be calculated from results of molecular orbital calculations

$$\Delta H°_{r,298} = \Delta E_{elec} + \Delta E_{ZPVE}(0) + \Delta E_{int}(298) + 5RT/2 \quad (3)$$

where ΔE_{elec}, $\Delta E_{ZPVE}(0)$, and $\Delta E_{int}(298)$ refer to the changes in electronic energy, zero-point vibrational energy, and thermal energy required to calculate reaction 1 at 298.15 K, respectively. The constant $5RT/2$ is the classical estimation of the effect of gaining three translational degrees of freedom ($3RT/2$) for the proton plus RT, the PV work term for the proton. The basicity can then be determined by substituting eq 3 into eq 2 with

$$T\Delta S_{r,298} = (298.15)(S(BH^+) - S(B)) - 7.8 \text{ kcal mol}^{-1} \quad (4)$$

where the constant 7.8 kcal mol^{-1} is the entropy of the proton at 298.15 K.

As shown earlier, for triglycine **N1** and **N2** have the lowest free energy (note, however, that **N1**, **N2**, and **N3** are all within 0.2 kcal mol^{-1} of one another) and for protonated triglycine structure **2** has the lowest free energy, although **4** is only 0.1 kcal mol^{-1} higher in energy. By using **N1** and **2**, the calculated *basicity* of triglycine is *216.3* kcal mol^{-1}. By using **N1** and **1** (protonation at the N-terminal amino group), the basicity is 215.0 kcal mol^{-1}. This latter basicity is to be compared with the previously calculated value of Zhang et al.,[11] who used the site of protonation as being the amino nitrogen and obtained a value of 219.6 kcal mol^{-1}, approximately 5 kcal mol^{-1} higher than our value. The experimental values of the basicities of GGG, together with an explanation of the methods used and their deficiencies, were recently revised and reviewed by Harrison.[27] The proton affinities, and also the basicities, were again revised by Strittmatter and Williams[12] using updated values for the reference bases. The revised basicities are 210.4 ± 4.0 kcal mol^{-1} from the reaction bracketing data of Wu and Lebrilla:[23a] 213.6 ± 2.9 kcal mol^{-1} from the reaction bracketing data of

Cassady and co-workers[24] and 216.6 ± 0.5 kcal mol^{-1} from the kinetic method data of Wu and Fenselau.[28] The last two experimental values are in good agreement with our calculated basicity of 216.3 kcal mol^{-1}. The first experimental result has an upper limit of 214.4 kcal mol^{-1}, a value within 1.9 kcal mol^{-1} of our calculated value.

Our calculated *proton affinity*, assuming **N1** forms **2**, is *223.8* kcal mol^{-1}. The value becomes 224.2 kcal mol^{-1}, if **N1** forms **1**. In comparison, Strittmatter and Williams[12] reported a calculated value of 227.8 kcal mol^{-1}, assuming the protonation site to be the amino nitrogen. The updated experimental values by the same authors[12] are 221.3 ± 4.0 kcal mol^{-1} with Wu and Lebrilla's data,[23a] 221.9 ± 2.9 kcal mol^{-1} with Cassady and co-workers' data,[24] and 224.7 ± 0.5 kcal mol^{-1} with Wu and Fenselau's data.[28] Our calculated proton affinity of 223.8 kcal mol^{-1} is within the error limits of the first two experimental values and 0.4 kcal mol^{-1} from the lower error limit of the third value.

Conclusions

The potential energy hypersurface for the fragmentation of protonated glycylglycylglycine to the b_2 ion and glycine has been calculated at the B3LYP/6-31++G(d,p) level of theory. The barrier to this fragmentation is about 33 kcal mol^{-1}. There are three structures with almost identical energies, separated by only 1.3 kcal mol^{-1}, in contention to be at the global minimum for protonated GGG. Of the three, the most favorable site of protonation is the N-terminal carbonyl oxygen where hydrogen bonding to the N-terminal nitrogen is stabilizing. In the structure at the second lowest energy minimum, protonation is at the carbonyl oxygen of the first residue, with hydrogen bonding to the carbonyl oxygen of the second residue providing stabilization. Protonation on the N-terminal amino group produces a structure at a minimum that is 1.3 kcal mol^{-1} (in free energy) above the lowest energy structure that we calculated. Hitherto, it has generally been accepted that protonation on the N-terminal nitrogen atom would provide the global minimum structure in polyglycines; however, our calculations here show this to be incorrect. Finally, density functional theory calculations at the B3LYP/6-31++G(d,p) level of theory yield gas-phase basicities and proton affinities that are within 1.2 kcal mol^{-1} of experimental values.

Acknowledgment. We would like to thank Professor Alex G. Harrison, for his many helpful discussions and for providing some of his preprints, and Steve Quan and John Saroglu, for expert technical assistance. A.C. would like to acknowledge NSERC for a graduate scholarship. We are grateful to NSERC for its continual support.

Supporting Information Available: Table giving the total electronic energies, zero-point vibrational energies, thermal energies, and entropies of structures (PDF). This material is available free of charge via the Internet at http://pubs.acs.org.

JA0015904

(26) (a) Wyttenbach, T.; Heldon, G. V.; Bowers, M. T. *J. Am. Chem. Soc*. **1996**, *118*, 8355−8364. (b) Wu, J.; Fenselau, C. *Int. J. Mass Spectrom. Ion Processes* **1991**, *111*, 173−189. (c) Wu, Z.; Fenselau, C. *Tetrahedron* **1993**, *49*, 9197−9206. (d) Campbell, S.; Rodgers, M. T.; Marzluff, E. M.; Beauchamp, J. L. *J. Am. Chem. Soc*. **1994**, *116*, 9765−9766. (e) Campbell, S.; Rodgers, M. T.; Marzluff, E. M.; Beauchamp, J. L. *J. Am. Chem. Soc.* **1995**, *117*, 12840−12854. (f) Nair, H.; Wysocki, V. H. *Int. J. Mass Spectrom. Ion Processes* **1998**, *174*, 95−100.

(27) Harrison, A. G. *Mass Spectrom. Rev.* **1997**, *16*, 201−217.

(28) Wu, Z.; Fenselau, C. *J. Am. Soc. Mass Spectrom*. **1992**, *3*, 863−866.